

Synthesis of Activated Carbon and MCM-41 from Bagasse and Rice Husk and their Carbon Dioxide Adsorption Capacity

A. Boonpoke^{1,3,4}, S. Chiarakorn², N. Laosiripojana^{1,4}, S. Towprayoon^{1,4} and A. Chidthaisong^{1,4,*}

¹The Joint Graduate School of Energy and Environment, King Mongkut's University of Technology Thonburi, Bangkok, Thailand

²Division of Environmental Technology, School of Energy, Environment and Materials, King Mongkut's University of Technology Thonburi, Bangkok, Thailand

⁴Center for Energy Technology and Environment, Bangkok, Thailand

³Current address: School of Energy and Environment, University of Phayao, Tumbol Maeka, Muang, Phayao 56000 Thailand

*Corresponding author: amnat_c@jgsee.kmutt.ac.th

Abstract: The aims of this work were to synthesize the porous solid adsorbents and to study their carbon dioxide (CO₂) adsorption capacities. Three adsorbents; activated carbon synthesized from bagasse (BAC) and from rice husk (RAC), and Mobil Composition of Matter number 41 (MCM-41) from rice husk silica (R-MCM-41) were investigated. The synthesized BAC, RAC and R-MCM-41 showed high thermal stability with the weight loss less than 0.1% for the temperatures below 150°C. N₂ adsorption isotherm analysis indicates that BAC and RAC are microporous while R-MCM-41 is mesoporous materials. The BET surface areas were 923, 927 and 602 m² g⁻¹ for BAC, RAC and R-MCM-41, respectively. The total pore volumes were 0.53, 0.56 and 0.49 cm³ g⁻¹, and pore sizes were 0.8, 0.8, and 2.43 nm for BAC, RAC and R-MCM-41, respectively. At 30°C these materials were able to adsorb 76.89, 57.13 and 23.32 mg-CO₂ g⁻¹-adsorbent, respectively. When the adsorption temperature increased, adsorption capacity of BAC, RAC and R-MCM-41 was decreased. This implied that physical process was the main mechanism of CO₂ adsorption.

Keywords: Activated carbon, MCM-41, Carbon dioxide, Adsorption, Rice husk and Bagasse.

1. Introduction

Global warming caused by increasing concentrations of greenhouse gases (GHGs) in the atmosphere is one of the emerging threats challenging mankind. Among GHGs, CO₂ is the biggest contributor to the current warming [1]. Mainly due to the emission from fossil fuels consumption, the atmospheric CO₂ concentrations have been increasing from the pre-industrial period of 280 ppmv to 380 ppmv in 2004 [2]. Among emission sources, fossil-fuel fired power plant for electricity generation is the biggest point source of atmospheric CO₂ [3]. To slow down GHGs concentrations in the atmosphere and therefore the global warming rate, urgent mitigation options are needed. Since it is one of the main contributors to global CO₂ emission, CO₂ separation from power plant's flue gas stack and sequestration in the safe location have been recommended as an immediate and effective CO₂ reduction mitigation option [2]. Consequently, many mitigation options potentially applied for CO₂ emission reduction have been proposed. These include improvement of the energy efficiency, uses of low carbon energy sources, and application of carbon dioxide capture and storage (CCS). The CCS system typically consists of CO₂ separation, transportation and long term isolation of captured CO₂ from the atmosphere. Based on existing CO₂ capture technology, adsorption by alkanolamines is the most widely used [4]. However, this process is only economically feasible when applied to the large post-combustion power plant. For the medium and small plants, the process relatively consumes high amount of energy (15-37% of the net power produced), and thus makes them economically not feasible [5]. In addition, the capture efficiency of amine usually decreases when heat-stable salts are formed during operation and when other interferences present in flue gas such as NO₂ and SO₂ [6].

Improving CO₂ adsorption efficiency, reducing cost and energy penalty in CO₂ capture process, therefore, will help reduce the overall cost and increase the possibility of implementing CCS as the emission mitigation options [7]. Adsorption by solid porous materials such as zeolites [8-9], SBA-15 [10-12], fly ashes [7], carbon nanotubes [13], MCM-48 [14], MCM-41 [15-16] and activated carbon [17-20] have been studied. Results among these varied depending on the characteristics of adsorbents.

For example, the CO₂ adsorption at 75°C of activated anthracites and AC-850-3-PEI were 28 and 26.3 mg-CO₂ g⁻¹-adsorbent, respectively [21]. Knofel et al. [22] studied CO₂ adsorption using SBA-15 silica synthesized from tri-block copolymer F127 and found that the adsorption capacity at 30 bars was 6.5 mmol g⁻¹ for non-grafted silica sample. Drage et al. [23] studied the preparation of CO₂ adsorbents from the chemical activation of urea-formaldehyde (UF) and melamine-formaldehyde (MF) resins. They showed that UF adsorbent obtained from chemical activation have the highest CO₂ adsorption capacity (0.08 g-CO₂ g⁻¹-adsorbent) at 25°C. For mesoporous material (MCM-41), the adsorption of 8.6 mg-CO₂ g⁻¹-adsorbent at 75°C was reported [15].

The results from these indicate that the porous materials have high potential for CO₂ adsorption. The CO₂ adsorption capacity, however, very much depends on temperatures and types of adsorbents. These are reflected in the detail characteristics of adsorbents such as pore sizes and their distribution, pore volume, and surface functional groups. These characteristics are in turned determined by the indigenous characteristics of raw materials (e.g. chemical composition) and by how they are synthesized into porous adsorbents.

Since they are highly porous and can be produced from biomass-based raw materials, activated carbon and MCM-41 are considered as those that are potentially used for CO₂ capture [21-24]. However, they have not yet been widely tested for CO₂ capture. Therefore, the aims of this paper were to synthesize the CO₂ adsorbents from the locally available biomass such as rice husk and bagasse, and to investigate their adsorption capacity. It is hoped that this will provide the material choices for effective CO₂ adsorption, which could be developed further to reduce the cost.

2. Experimental

2.1 Activated carbon synthesis

Bagasse used in this experiment was obtained from the sugar factory located in Suphanburi province, central part of Thailand (Mitr Phol Sugar Group Thailand). Rice husk was given by the Drying Technology Laboratory at King Mongkut's University of Technology Thonburi (KMUTT), Thailand. After washing with deionized water, the raw materials were oven-

dried at 80°C for 24 h. The method of activated carbon synthesis was modified from Tsai et al. [25] and Önal et al. [26]. The raw material was mixed with ZnCl₂ (assay 95%, Ajax Finechem, New Zealand) at the weight ratio of 1:1 for 1 h and dried at 105°C for 24 h. The sample was carbonized using horizontal furnace with a 46 mm diameter quartz reactor. The carbonization was carried out by heating at the rate of 10°C min⁻¹ from room temperature up to 500°C and hold at that temperature for 1 h under N₂ flow (100 ml min⁻¹). The sample was then cooled to room temperature. The residual activation reagent was removed from the sample by using 0.5N HCl [27]. The resulting BAC and RAC were washed with hot distilled water several times to remove residual chloride ions. Finally, the activated carbon was dried using reduced pressure vacuum oven (Memmert, VO 500, Germany) at 70°C, at 700 mmHg for 24 h.

2.2 Rice husk silica extraction and R-MCM-41 synthesis

Rice husk silica extraction was carried out using acid hydrolysis method modified from Yalçın and Sevinç [28] and Chiarakorn and Saprom [29]. Firstly, rice husk was washed by distilled water and dried at 80°C for 24 h. Secondly, the sample was hydrolyzed with 1 M HCl at 80°C for 1 h. The hydrolyzed sample was rinsed with distilled water until pH reached 7, then dried at 105°C for 24 h. Finally, the sample was calcined at 650°C for 4 h using muffle furnace (JSMF-30T, JSR, South Korea).

The extracted rich husk silica (RHS) was then used for R-MCM-41 synthesis. The details of synthesis procedure were described by Chiarakorn et al. [30]. RHS was mixed with hexadecyltrimethyl ammonium bromide (CTAB) at the molar composition ratio of 1.0 SiO₂: 1.09 NaOH: 0.13 CTAB: 0.12 H₂O. The pH of the mixture was kept at 10. After continuous stirring for 48 h, the suspended solid was filtered and rinsed with ethanol and distilled water, and finally calcined at 550°C for 5 h.

2.4 BAC, RAC and R-MCM-41 characterization

Proximate analysis was performed using thermogravimetric analyzer (TGA: Pyris 1 TGA, Perkin Elmer, Massachusetts, USA). The proximate analysis provides the relative amounts of moisture, volatile matter, fixed carbon, and ash content. All proximate analysis in this work was reported on dry basis. Typically, 10 mg (particle size less than 75 micron) of biomass was placed into the small platinum sample holder. The sample was heated from 30°C up to 900°C under N₂ atmosphere. An air zero was introduced instead of N₂ and hold for 10 min at the final step to obtain the ash content. The weight loss during pyrolysis was calculated to the percentage of volatile matter, and fixed carbon. In addition fixed carbon was calculated by weight fraction basis (fixed carbon = 1 - ash - volatile matter). The chemical elemental composition (CHNS) of biomass and activated carbon were examined by using an elemental analyzer (Thermo Finnigan, Flash EA 1112, USA). The analytical procedure was followed the protocols provided by manufacturer. The oxygen percentage was obtained by subtracting from the sum of C, H, N, and S.

Porosity was determined by studying N₂ adsorption isotherm at -196.15°C using BELSORP-mini II, (BEL Japan Inc). According to manufacturer recommendation, this method is based on the assumption that adsorbed N₂ at liquid N₂ temperature has a hexagonal cross sectional area of 0.162 nm². The surface area was calculated using the Brunauer-Emmett-Teller (BET) equation.

The materials were examined their crystalline property using X-ray diffraction spectrometer (D-8 Discover, Bruker, U.S.A.). The X-ray diffraction (XRD) patterns were obtained using CuK α radiation source (40 kV, 40 mA).

2.5 Carbon dioxide adsorption

The adsorption/desorption experiment was carried out using TGA over the adsorption temperatures ranges from 30 to

150°C. The experimental procedure was adapted from Xu et al. [15], Mercedes Maroto-Valer et al. [21] and Plaza et al. [31]. Typically, 10 mg of adsorbent was placed into a small platinum pan, heated up to 110°C under N₂ flow (fixed gas flow rate at 50 ml min⁻¹ was used through out this work) and hold for 30 min. Then, the temperature was decreased (adsorption temperature of 30-100°C) or increased (adsorption temperature of 125-150°C) to the desired adsorption temperatures. The adsorption capacity was studied by introducing 99.9% purity of CO₂ to adsorption chamber until no weight change. After the adsorption reached to the equilibrium, the desorption was carried out by switching the gas from CO₂ to N₂. The stability of CO₂ adsorption performance of adsorbents was examined at the temperature of 50°C by repeating adsorption/desorption for seven cycles. The CO₂ adsorption capacity was reported as mg-CO₂ g⁻¹-adsorbent.

3. Results and Discussion

3.1 Materials characteristics

3.1.1 Thermogravimetric, proximate and ultimate analysis

The thermogravimetric analysis of the produced activated carbon as a function of temperature is shown in Figure 1. It can be seen that BAC and RAC are stable at relatively high heating temperature. At the temperature of 150°C, the accumulated weight loss of BAC and RAC was very small as 0.11 and 0.09 wt%, respectively. Typically, the temperature of flue gas from power plant is in the range of 70-150°C, thus BAC and RAC should be feasible for using in power plant stack. It is noted that at higher temperature, i.e. at 650°C, more weight loss was observed. Önal et al. [26] suggested that such phenomenon was caused by conversion of residual lignin to carbon monoxide. The carbon content of activated carbon was also reduced by high heating temperature, producing carbon monoxide. The accumulated weight loss of BAC and RAC up to 500°C was 2.53 and 2.32 wt%, respectively. In contrast to BAC and RAC, the weight loss of R-MCM-41 was negligible (<0.03%) throughout the temperature range of 30-900°C. The XRD pattern of R-MCM-41 indicates its crystalline structure and a uniform hexagonal arrangement (data not shown). This implies that structure of R-MCM-41 is highly thermal stable and thus could be potentially used as adsorbent at high temperature [30].

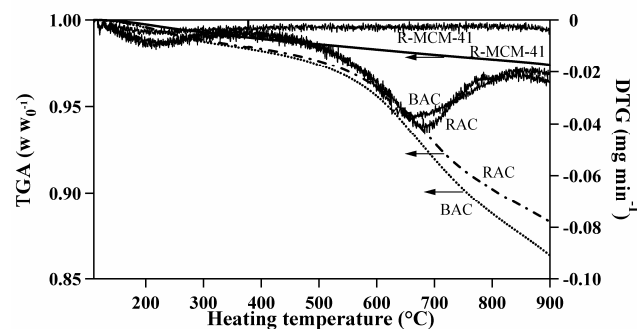


Figure 1. TGA and DTG of BAC, RAC and R-MCM-41 as a function of temperature.

The proximate and ultimate properties of the raw materials and the produced activated carbons are shown in Table 1. The major components of raw materials are volatile matter and fixed carbon. The main features of these materials and RAC show high ash contents. After carbonization, the fixed carbon fraction of BAC (84.5 wt.%) and RAC (62.8 wt.%) was obviously higher than the raw materials (10.5 and 15.8 wt.% for bagasse and rice husk, respectively). Relatively low fixed carbon content of RAC compared to BAC may be due to the fact that rice husk is composed of minerals such as silicon and other trace minerals which can not be removed at carbonized temperature of 500°C.

Table 1. Characteristics of raw materials and the synthesized adsorbents.

Property	Bagasse	Rice husk	BAC	RAC	R-MCM-41
Proximate analysis (wt.%)					
Fixed carbon	10.5	15.8	84.5	62.8	na
Volatile	83.3	67.5	13.6	11.8	na
Ash	6.2	16.7	1.9	25.4	na
Ultimate analysis (wt.%)					
C	41.55	36.52	64.12	54.75	na
H	5.55	4.82	1.25	1.31	na
N	0.03	0.86	0.34	0.50	na
O	52.86	41.10	34.29	18.04	na
BET surface area (m ² g ⁻¹)	na	na	923	927	602
Pore volume (cm ³ g ⁻¹)	na	na	0.53	0.56	0.49
Porosity (%) [*]	na	na	99.19	96.22	na
Pore size (nm)	na	na	0.80	0.80	2.43

na = not analyzed

^{*} Porosity is the ratio of micropore volume to total pore volume

From these results it can be concluded that the synthesis process successfully enhance the relative carbon proportion of the materials that could be effectively used as the precursors of activated carbon synthesis [32-37].

3.1.2 Surface area, pore size distribution and porosity

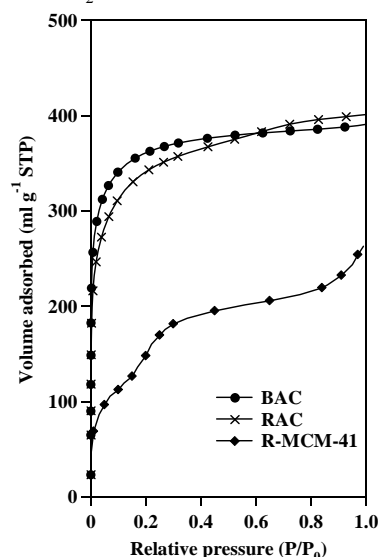
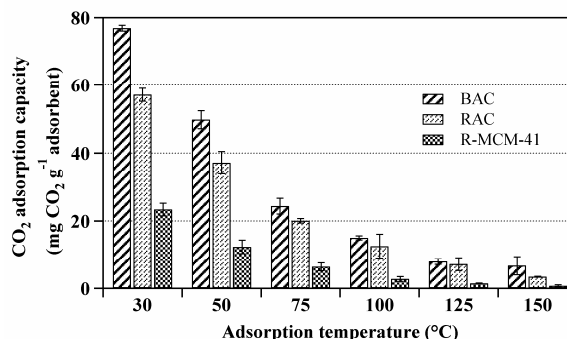
N₂ adsorption isotherm was carried out to study physical property of activated carbons and R-MCM-41 (Figure 2). Both BAC and RAC exhibited type I adsorption isotherm according to the International Union of Pure and Applied Chemistry (IUPAC) classification [38]. The adsorption isotherm implies that the activated carbons are microporous (micropore: width less than 2 nm, mesopore: width from 2 to 50 nm, macropore: width greater than 50 nm). The pore filling took place at relative low pressure, and was higher for BAC than RAC up to the relative pressure at around 0.6, indicating the higher adsorption potential for BAC over that pressure ranges. At the relative pressure higher than 0.6, the filling rate for RAC was better than for BAC. This might be due to the different pore characteristics such as pore size distribution and pore shape. The results agree well with the porosity analysis that BAC had higher porosity than RAC (99.19% for BAC vs. 96.22% for RAC). On the other hand, N₂ adsorption isotherm indicates that R-MCM-41 falls within type IV isotherm. The pattern of N₂ filling indicates the capillary condensation in response to the presence of mesopore. At any given relative pressure, the filling rate of R-MCM-41 was significantly lower than that of activated carbon, suggesting the relatively low adsorption capacity. This can be explained by the fact that surface of R-MCM-41 is largely made up of the polar silanol group (Si-OH), and thus not effective in adsorbing the non-polar molecules such as N₂. However, R-MCM-41 has the advantages of very high heat stability as mentioned above.

The BET surface areas of BAC, RAC and R-MCM-41 were 923, 927 and 602 m² g⁻¹, respectively. This is consistent with the pore size analysis that both BAC and RAC are microporous and R-MCM-41 is mesoporous (Table 1), and the N₂ isotherm shown in Figure 2.

3.2 Carbon dioxide adsorption capacity

The CO₂ adsorption capacity of BAC, RAC and R-MCM-41 at various adsorption temperatures is shown in Figure 3. At 30°C, BAC provided the highest adsorption capacity of 76.89, followed by RAC and R-MCM-41 of 57.13 and 22.40 mg-CO₂ g⁻¹-adsorbent, respectively. At any given temperature, BAC showed the highest adsorption capacity. Despite the similar surface area and pore characteristics, RAC had lower adsorption capacity than BAC. As mentioned above, the main differences are its significant higher ash and lower carbon content. Higher ash content indicates the existence of certain mineral components that may reduce RAC adsorption capacity. In addition, the higher microporosity of BAC than RAC (99.19% and 96.22%,

respectively) may play the important roles. According to Mercedes Maroto-Valer et al. [21], one of their samples with lower surface area (540 m²g⁻¹) had higher CO₂ adsorption capacity (65.7 mg-CO₂ g⁻¹-adsorbent) when compared to that of the anthracite (40.0 mg-CO₂ g⁻¹-adsorbent) which had the higher surface area and pore volume (1071 m² g⁻¹ and 0.558 cm³ g⁻¹, respectively). They suggested that not all the surface area or the pore volume of the activated anthracites contributes to the adsorption of the CO₂.

**Figure 2.** N₂ adsorption isotherms of BAC, RAC and R-MCM-41.**Figure 3.** CO₂ Adsorption capacity of BAC, RAC and R-MCM-41 at different adsorption temperatures.

At the ambient atmospheric pressure, it is suggested that the effective pore size to capture the gas is only the pore size smaller than 5 times of the adsorbate molecular sizes [21]. The CO₂ molecular size (liquid phase in nanopore material) is 0.209 nm. Therefore the effective pore size to capture CO₂ is pore size

smaller than 1.0 nm. In addition, Vishnyakov et al. [39] reported that based on Grand Canonical Monte Carlo (GCMC) simulations and the Non-Local Density Functional Theory (NLDFT), the pore size smaller than 0.26 nm is too narrow for CO₂ adsorption. In this study, the average pore size of R-MCM-41 was 2.43 nm, which is bigger than the effective size. Together with its relatively low surface area, this may be the reason that the adsorption capacity of R-MCM-41 was quite low.

For the temperature range of 30–150°C, CO₂ adsorption capacity decreased as adsorption temperature increased. The relationship between adsorption and temperatures is given in Figure 4. Generally, the adsorption capacity of BAC, RAC, R-MCM-41 significantly correlated ($P < 0.05$) with temperatures. The adsorption exponentially decreased as temperature increased, and can be generally expressed as $y = ae^{-kt}$, where y is adsorption capacity in mg of CO₂ per gram of adsorbent, and t is adsorption temperature. Among the adsorbent tested, the rate of decreasing adsorption capability with increasing temperature was similar between BAC and RAC, but different from R-MCM-41. The adsorption capacity of BAC, RAC and R-MCM-41 at 30°C was about 11, 17 and 32 times higher than that of at 150°C, respectively. Thus, CO₂ adsorption by R-MCM-41 was the most sensitive to temperature.

The dependency of adsorption on temperature is a well-known characteristic of physical adsorption. This adsorption behaviors is similar to others studies using carbon nanotubes [13], commercial activated carbon [40], activated anthracite [21] and MCM-41 [15]. In addition, Van Der Vaart et al. [41] reported that the CO₂ adsorption of Nortit RBI activated carbon was decreased from 108 to 40 mg-CO₂ g⁻¹-adsorbent when the adsorption temperature was increased from 21.5 to 75°C.

Table 2 shows the adsorption capacity obtained from synthesized activated carbons and R-MCM-41 compared to the results available in the literatures. At 30°C, adsorption capacity of both BAC and RAC is highest among the lists. However, all solid sorbents showed similar adsorption behavior, the adsorption capacity decreased with the increasing of adsorption temperature.

Table 2. CO₂ adsorption capacity of the synthesized adsorbents compared to those available from literatures (mg-CO₂ g⁻¹-adsorbent).

Adsorbent	Adsorption capacity (mg-CO ₂ g ⁻¹ -adsorbent)			References
	30°C	75°C	150°C	
BAC	76.89	24.30	6.73	This work
FA2 ^{a)}	17.5	10.2	-	[24]
FA2-DEM ^{b)}	43.5	22.0	-	[24]
RAC	57.13	20.03	3.45	This work
Activated anthracite	58	28	-	[21]
AC-850-3-PEI ^{c)}	-	26.3	-	[21]
R-MCM-41	23.32	6.42	0.73	This work
Si-MCM-41	-	8.6	-	[15]

^{a)} Fly ashes

^{b)} de-ashed fly ashes

^{c)} AC-850-3-PEI is activated anthracite at 850°C for 3 h, and impregnated with polyethylenimine (PEI) as 33.5 wt.%

3.3 Reuse potential

Another aspect of desirable adsorbent is its ability to be reused or regenerated. This was tested at 50°C (Figure 5). The results indicate that all adsorbents can be reused several times. The average CO₂ adsorption capacity for seven cycles of use was 49.05±1.31, 36.72±2.01 and 9.59±0.24 mg-CO₂ g⁻¹-adsorbent for BAC, RAC and R-MCM-41 respectively. Significantly lower variation for R-MCM-41 indicates its advantages over activated carbon for reusability. This agrees well with its high thermal stability as mentioned above. Thus, although R-MCM-41 has lower CO₂ adsorption capacity, but there are some desirable features that could be developed further to enhance its adsorption ability.

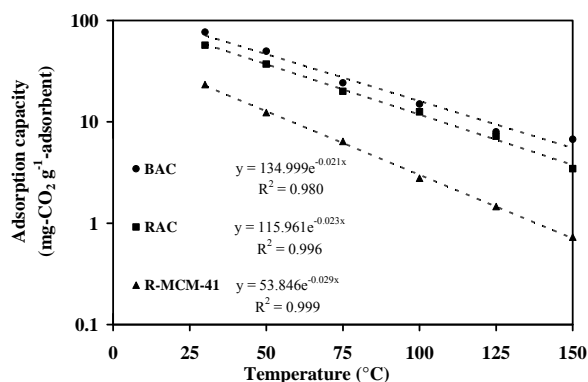


Figure 4. Relationship between adsorption capacity and temperatures of BAC, RAC and R-MCM-41.

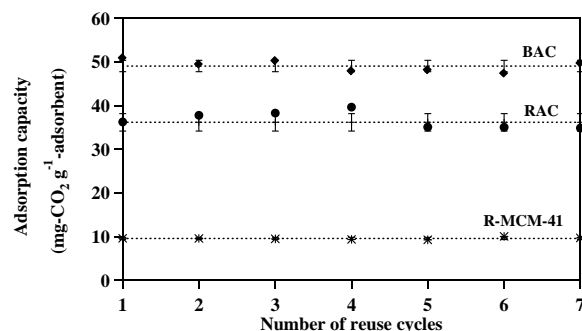


Figure 5. Variations in adsorption capacities when the adsorbents were repeatedly used at 50°C.

4. Conclusions

This study used rice husk and bagasse as raw materials for activated carbon and R-MCM-41 synthesis. The synthesized rice husk and bagasse activated carbon (RAC and BAC, respectively) is of micropore with the average pore size of 0.8 nm. On the other hand, rice husk MCM-41 (R-MCM-41) is of mesopore, with the average pore size of 2.3 nm. Among these adsorbents, BAC shows the highest capacity of CO₂ adsorption. Its high adsorption capacity is related to its high surface area, high carbon content, and low ash content. For all adsorbents synthesized in this study, their CO₂ adsorption is negatively correlated with the temperature. As temperature becomes higher, differences in adsorption capacity among the adsorbents diminishes. This indicates that physical adsorption is the dominated adsorption mechanism. The capacity of the synthesized adsorbents is relatively higher when compared to the similar classes of adsorbents in the literatures, indicating their high potentials to be developed further for CO₂ adsorption.

Acknowledgements

This work was financially supported by the National Metal and Materials Technology Center (MTEC), Thailand, Shell Centenary Scholarship Foundation and The Joint Graduate School of Energy and Environment and the Commission of Higher Education's Center for Energy Technology and Environment, King Mongkut's University of Technology Thonburi.

References

- [1] Pachauri RK, Reisinger A, *Climate Change 2007: Synthesis Report* (2007).
- [2] Metz B, Ogunlade D, Connink H, Loos M, Meyer L, *Special Report on Carbon Dioxide Capture and Storage* (2005) Cambridge University Press.

- [3] IPCC, *Climate Change 2007: The Physical Science Basis. Contribution of Working Group I to the Fourth Assessment Report of the Intergovernmental Panel on Climate Change* (2007).
- [4] Zhao H, Hu J, Wang J, Zhou L, Liu H, CO₂ Capture by the Amine-modified Mesoporous Materials, *Acta Physico-Chimica Sinica* 23 (2007) 801-806.
- [5] Grande CA, Rodrigues AE, Electric Swing Adsorption for CO₂ removal from flue gases, *International Journal of Greenhouse Gas Control* 2 (2008) 194-202.
- [6] Arenillas A, Smith KM, Drage TC, Snape CE, CO₂ capture using some fly ash-derived carbon materials, *Fuel* 84 (2005) 2204-2210.
- [7] Gray ML, Soong Y, Champagne KJ, Baltrus J, Stevens RW, Toochinda P, Chuang SSC, CO₂ capture by amine-enriched fly ash carbon sorbents, *Separation and Purification Technology* 35 (2004) 31-36.
- [8] Katoh M, Yoshikawa T, Tomonari T, Katayama K, Tomida T, Adsorption Characteristics of Ion-Exchanged ZSM-5 Zeolites for CO₂/N₂ Mixtures, *Journal of Colloid and Interface Science* 226 (2000) 145-150.
- [9] Siriwardane RV, Shen MS, Fisher EP, Losch J, Adsorption of CO₂ on Zeolites at Moderate Temperatures, *Energy Fuels* 19 (2005) 1153-1159.
- [10] Liu X, Zhou L, Fu X, Sun Y, Su W, Zhou Y, Adsorption and regeneration study of the mesoporous adsorbent SBA-15 adapted to the capture/separation of CO₂ and CH₄, *Chemical Engineering Science* 62 (2007) 1101-1110.
- [11] Zhao Z, Cui X, Ma J, Li R, Adsorption of carbon dioxide on alkali-modified zeolite 13X adsorbents, *International Journal of Greenhouse Gas Control* 1 (2007) 355-359.
- [12] Gray ML, Soong Y, Champagne KJ, Pennline H, Baltrus JP, Stevens JRW, Khatri R, Chuang SSC, Filburn T, Improved immobilized carbon dioxide capture sorbents, *Fuel Processing Technology* 86 (2005) 1449-1455.
- [13] Su F, Lu C, Cnen W, Bai H, Hwang JF, Capture of CO₂ from flue gas via multiwalled carbon nanotubes, *Science of The Total Environment* 407 (2009) 3017-3023.
- [14] Jang HT, Park Y, Ko YS, Lee JY, Margandan B, Highly siliceous MCM-48 from rice husk ash for CO₂ adsorption, *International Journal of Greenhouse Gas Control* 3 (2009) 545-549.
- [15] Xu X, Song C, Andresen JM, Miller BG, Scaroni AW, Preparation and characterization of novel CO₂ "molecular basket" adsorbents based on polymer-modified mesoporous molecular sieve MCM-41, *Microporous and Mesoporous Materials* 62 (2003) 29-45.
- [16] Xu X, Song C, Andresen JM, Miller BG, Scaroni AW, Novel Polyethylenimine-Modified Mesoporous Molecular Sieve of MCM-41 Type as High-Capacity Adsorbent for CO₂ Capture, *Energy Fuels* 16 (2002) 1463-1469.
- [17] Guo B, Chang L, Xie K, Adsorption of Carbon Dioxide on Activated Carbon, *Journal of Natural Gas Chemistry* 15 (2006) 223-229.
- [18] Sarkar SC, Bose A, Role of activated carbon pellets in carbon dioxide removal, *Energy Conversion and Management* 38 (1997) S105-S110.
- [19] Sun Y, Wang Y, Zhang Y, Zhou Y, Zhou L, CO₂ sorption in activated carbon in the presence of water, *Chemical Physics Letters* 437 (2007) 14-16.
- [20] Pellerano M, Pré P, Kacem M, Delebarre A, CO₂ capture by adsorption on activated carbons using pressure modulation, *Energy Procedia* 1 (2009) 647-653.
- [21] Mercedes Maroto-Valer M, Tang Z, Zhang Y, CO₂ capture by activated and impregnated anthracites, *Fuel Processing Technology* 86 (2005) 1487-1502.
- [22] Knofel C, Descarpentries J, Benzaouia A, Zelenak V, Mornet S, Llewellyn PL, Hornebecq V, Functionalised micro-/mesoporous silica for the adsorption of carbon dioxide, *Microporous and Mesoporous Materials* 99 (2007) 79-85.
- [23] Drage TC, Arenillas A, Smith KM, Pevida C, Piippo S, Snape CE, Preparation of carbon dioxide adsorbents from the chemical activation of urea-formaldehyde and melamine-formaldehyde resins, *Fuel* 86 (2007) 22-31.
- [24] Mercedes Maroto-Valer M, Lu Z, Zhang Y, Tang Z, Sorbents for CO₂ capture from high carbon fly ashes, *Waste Management* 28 (2008) 2320-2328.
- [25] Tsai WT, Chang CY, Lee SL, A low cost adsorbent from agricultural waste corn cob by zinc chloride activation, *Bioresource Technology* 64 (1998) 211-217.
- [26] Önal Y, Akmil-Başar C, Sarici-Özdemir Ç, Erdogan S, Textural development of sugar beet bagasse activated with ZnCl₂, *Journal of Hazardous Materials* 142 (2007) 138-143.
- [27] Namasivayam C, Sangeetha D, Kinetic studies of adsorption of thiocyanate onto ZnCl₂ activated carbon from coir pith, an agricultural solid waste, *Chemosphere* 60 (2005) 1616-1623.
- [28] Yalçın N, Sevinç V, Studies on silica obtained from rice husk, *Ceramics International* 27 (2001) 219-224.
- [29] Chiarakorn S, Saprom Y, *Structure of Mesoporous MCM-41 Prepared from Rice Husk Ash* (2005) The 8th Asian Symposium on Visualization, Chaingmai, Thailand.
- [30] Chiarakorn S, Areerob T, Grisdanurak N, Influence of functional silanes on hydrophobicity of MCM-41 synthesized from rice husk, *Science and Technology of Advanced Materials* 8 (2007) 110-115.
- [31] Plaza MG, Pevida C, Arenillas A, Rubiera F, Pis JJ, CO₂ capture by adsorption with nitrogen enriched carbons, *Fuel* 86 (2007) 2204-2212.
- [32] Gupta VK, Mittal A, Jain R, Mathur M, Sikarwar S, Adsorption of Safranin-T from wastewater using waste materials- activated carbon and activated rice husks, *Journal of Colloid and Interface Science* 303 (2006) 80-86.
- [33] Chuah TG, Jumariah A, Azni I, Katayon S, Thomas Choong SY, Rice husk as a potentially low-cost biosorbent for heavy metal and dye removal: an overview, *Desalination* 175 (2005) 305-316.
- [34] Yalçın N, Sevinç V, Studies of the surface area and porosity of activated carbons prepared from rice husks, *Carbon* 38 (2000) 1943-1945.
- [35] Mohan D, Singh KP, Single- and multi-component adsorption of cadmium and zinc using activated carbon derived from bagasse—an agricultural waste, *Water Research* 36 (2002) 2304-2318.
- [36] Guo Y, Yang S, Fu W, Qi J, Li R, Wang Z, Xu H, Adsorption of malachite green on micro- and mesoporous rice husk-based active carbon, *Dyes and Pigments* 56 (2003) 219-229.
- [37] Syna N, Valix M, Assessing the potential of activated bagasse as gold adsorbent for gold-thiourea, *Minerals Engineering* 16 (2003) 511-518.
- [38] Sing KSW, Everett DH, Haul RAW, Moscou L, Pierotti RA, Rouquerol J, Siemieniowska T, Reporting Physisorption Data for Gas/Solid Systems with Special Reference to the Determination of Surface Area and Porosity, *Pure Appl Chem* 57 (1985) 603-619.
- [39] Vishnyakov A, Ravikovitch PI, Neimark AV, Molecular Level Models for CO₂ Sorption in Nanopores, *Langmuir* 15 (1999) 8736-8742.
- [40] Pevida C, Plaza MG, Arias B, Feroso J, Rubiera F, Pis JJ, Surface modification of activated carbons for CO₂ capture, *Applied Surface Science* 254 (2008) 7165-7172.
- [41] Van Der Vaart R, Huiskes C, Bosch H, Reith T, Single and Mixed Gas Adsorption Equilibria of Carbon Dioxide/Methane on Activated Carbon, *Adsorption* 6 (2000) 311-323.